Available online at www.sciencedirect.com
ScienceDirect
Journal of Solid State Chemistry 180 (2007) 3218–3223
JOURNAL OF SOLID STATE CHEMISTRY
www.elsevier.com/locate/jssc

A highly coercive carbon nanotube coated with $Ni_{0.5}Zn_{0.5}Fe_2O_4$ nanocrystals synthesized by chemical precipitation–hydrothermal process

Huiqun Cao[b], Meifang Zhu[a,*], Yaogang Li[a], Jianhong Liu[b], Zhuo Ni[b], Zongyi Qin[a]

[a]*College of Material Science and Engineering, State Key Laboratory for Modification of Chemical Fibers and Polymer Material, Donghua University, Shanghai 200051, PR China*

[b]*College of Chemistry and Chemical Engineering, Shenzhen University, Shenzhen 518060, PR China*

Received 12 June 2007; received in revised form 23 August 2007; accepted 28 August 2007
Available online 1 September 2007

Abstract

Novel magnetic composites ($Ni_{0.5}Zn_{0.5}Fe_2O_4$–MWCNTs) of multi-walled carbon nanotubes (MWCNTs) coated with $Ni_{0.5}Zn_{0.5}Fe_2O_4$ nanocrystals were synthesized by chemical precipitation–hydrothermal process. The composites were characterized by X-ray powder diffractometer (XRD), X-ray photoelectron spectrometer (XPS), Fourier transform infrared spectroscopy (FTIR), Mössbauer spectroscopy (MS), transmission electron microscopy (TEM), and selected area electron diffraction (SAED), etc. A temperature of about 200 °C was identified to be an appropriate hydrothermal condition to obtain $Ni_{0.5}Zn_{0.5}Fe_2O_4$–MWCNTs, being lower than the synthesis temperature of a single-phase $Ni_{0.5}Zn_{0.5}Fe_2O_4$ nanocrystals. The sizes of $Ni_{0.5}Zn_{0.5}Fe_2O_4$ in the composites were smaller than those of $Ni_{0.5}Zn_{0.5}Fe_2O_4$ nanocrystals in single phase. The composites exhibited more superparamagnetic than $Ni_{0.5}Zn_{0.5}Fe_2O_4$ nanocrystals in their relaxation behaviors. The magnetic properties measured by a vibrating sample magnetometer showed that the composites had a high coercive field of 386.0 Oe at room temperature, higher than those of MWCNT and $Ni_{0.5}Zn_{0.5}Fe_2O_4$ nanocrystals.

Keywords: Carbon nanotubes; Coating; Chemical treatment; Magnetic properties; Mössbauer spectroscopy

1. Introduction

Nanostructural magnetic materials have unique properties, which are not showed by the bulk materials [1,2]. The composites consisting of magnetic media and electronic media are known as magnetoelectric materials. The materials exhibit electromagnetic properties and magnetoelectric effects, which are absent in the corresponding constituent phases [3–7]. Carbon nanotubes (CNTs) have been drawn a considerable attention for their unique electrical and mechanical properties due to promising versatile applications [8,9]. The combination of magnetic nanostructural materials and CNTs possibly resulting in high electronic or magnetic properties is highly attractive for new material development. In addition, hollow one-dimensional structural characteristics of CNTs may have many potential and important applications in magnetic data storage devices, magnetic stirrers of microfluidic devices and magnetic valves of nanofluidic devices [10,11].

Synthesis works of CNTs magnetic composites are reported in literatures [12–28]. Most of these investigations had been focused on the CNTs filled with magnetic nanomaterials [12–22], some studies on coating or attaching CNTs with magnetic nanocrystals were reported recently [23–28]. Jiang and Gao [23] reported that multi-walled CNT (MWCNT) coated with magnetite resulted in an increasing electrical conductivity of the composite. Vasilios et al. [24] attached magnetic nanoparticles on CNTs and synthesized soluble derivatives. However, there is no investigation on magnetic properties of the composites. Correa-Duarte et al. [25], coating CNTs with iron oxide nanoparticles in the way of polymer wrapping and layer-by-layer assembly then aligning magnetic CNTs

*Corresponding author. Fax: +86 21 62193062.
E-mail address: zmf@dhu.edu.cn (M. Zhu).

0022-4596/$ - see front matter © 2007 Elsevier Inc. All rights reserved.
doi:10.1016/j.jssc.2007.08.018

under low magnetic fields, achieved the magnetic function and showed superparamagnetic behavior at 5 K. He et al. [26] prepared the MWCNT–Fe^{2+} composite with coercive field of 260 Oe at 5 K. Jang et al. [27] prepared γ-Fe_2O_3-impregrated magnetic CNTs using polymer nanotubes as the carbon precursor, the magnetization curve exhibited typical ferromagnetic behavior, the saturation magnetization is ca. 3 emu/g and the coercivity is 226.17 Oe. Furthermore, Jang and Yoon [28] fabricated magnetic carbon nanotubes using a metal-impregnated polymer precursor. The author previously reported that decorated MWCNTs with iron oxide in coercive field of 163.4 Oe and a saturation magnetization of 20.1 emu/g at room temperature [29]. This work aims to an appropriate technique to prepare magnetic CNT composite with much higher coercivity in comparison with iron oxide/MWCNTs.

NiZn-ferrites have good magnetic properties, chemical stability, corrosion resistance, and reasonable cost [30,31], being extensively applied in information storage systems, medical diagnostics, and shielding against electromagnetic radiation. Liu and Gao [32] prepared CNTs–$NiFe_2O_4$ composites by hydrothermal process for the advantages of high purity, chemical homogeneity, uniform particle size, and low cost. The electrical conductivity of the composite was increased by 5 orders of magnitude on the basis of $NiFe_2O_4$. However, the magnetic properties of composites are not studied. It is well known that zinc can be used to improve the saturation magnetization; the addition of zinc also increases the lattice parameter, resulting in reduction of Curie temperature of the material [33]. The MWCNTs coated with Ni–Zn ferrite nanocrystals could be potentially multifunctional composite. However, the magnetic properties of the $Ni_{0.5}Zn_{0.5}Fe_2O_4$ attaching on the outside wall of MWCNTs were not reported. In this paper, MWCNTs are modified with nitric acid then coated with $Ni_{0.5}Zn_{0.5}Fe_2O_4$ nanocrystals by simple but efficient chemical precipitation–hydrothermal process. Furthermore, it is compared with $Ni_{0.5}Zn_{0.5}Fe_2O_4$ nanocrystals for the magnetic properties, as well as the microstructures of $Ni_{0.5}Zn_{0.5}Fe_2O_4$–MWCNTs. Intensive investigation reveals that the coercivity of $Ni_{0.5}Zn_{0.5}Fe_2O_4$–MWCNTs is higher than that of $Ni_{0.5}Zn_{0.5}Fe_2O_4$ nanocrystals.

2. Experimental

MWCNTs (diameters: 20–40 nm, purity: 95–98%) prepared by the catalytic decomposition of CH_4 were provided by Shengzhen Nanotech Port Ltd. Co. (China). The MWCNTs were washed in the solution of hydrofluoric acid, nitric acid, and distilled water, respectively, then filtered and dried at 100 °C to remove the catalyst residue and the impurity. The purified MWCNTs were oxidized by refluxing at 120 °C in concentrated nitric acid for 4.5 h. After the solution was cooled to room temperature, the oxidized MWCNTs were obtained by filtering, drying, and grinding. Stock solutions (1 M) of $Ni(NO_3)_2$, $Zn(NO_3)_2$, and $Fe(NO_3)_3$ were prepared. Different amounts of metal nitrate solutions were weighted to make various compositions of $Ni_{0.5}Zn_{0.5}Fe_2O_4$ precursors. The oxidized MWCNTs were added slowly into the precursor under vigorous agitation. The pH was adjusted using 6 M sodium hydroxide solutions. When the pH reached 10, the desired hydroxides were precipitated and the neutralization process was completed. A certain amount of distilled water was added into the precipitated hydroxides to make slurry, which was then subjected to hydrothermal treatment at different temperatures for 1–5 h in a Teflon-lined autoclave. The composites were cooled to room temperature, washed by distilled water until the sodium was completely removed. A final wash is performed using ethanol then dried at 100 °C for 12 h.

X-ray powder diffractometer (XRD) (D/max 2550V, Rigaku, Japan) with Cu $K\alpha$ radiation ($\lambda = 0.15406$ nm) was used to measure the structure of $Ni_{0.5}Zn_{0.5}Fe_2O_4$ nanocrystals. The sizes of $Ni_{0.5}Zn_{0.5}Fe_2O_4$ in composites and $Ni_{0.5}Zn_{0.5}Fe_2O_4$ nanocrystals were calculated based on XRD linewidth. VGESCALAB MK II X-ray photoelectron spectrometer (XPS) was applied to measure the surface element binding energy and chemical composition of the composites and MWCNTs samples. Fourier transform infrared spectroscopy (FTIR, NEXUS, Nicolet) was used to study chemical structure changes. Mössbauer spectroscopy (MS, Wissel, Germany) was used to study detailed structures using a source of ^{57}Co in a Pd matrix at room temperature. The velocity transducer was operated in a constant-acceleration mode. Hyperline interaction parameters can be obtained from the Mössbauer spectra using least-squares method. The morphologies were observed by transmission electron microscopy (TEM) (JEM 2010, JEOL, Japan) in an accelerating voltage of 200 kV. High-resolution TEM (HRTEM) images and selected area electron diffraction (SAED) were taken on the JEM2010. The magnetic properties were measured by a vibrating sample magnetometer (VSM, LH-3, China) in the magnetic field of 4 kOe at room temperature, including coercivity (H_c), saturation magnetization (M_s), and remanent magnetization (M_r), etc.

3. Results and discussion

Fig. 1 shows XRD patterns of $Ni_{0.5}Zn_{0.5}Fe_2O_4$ and MWCNTs coated with $Ni_{0.5}Zn_{0.5}Fe_2O_4$ ($Ni_{0.5}Zn_{0.5}Fe_2O_4$–MWCNTs) subjected to hydrothermal treatment at various conditions. Curve a is XRD pattern of $Ni_{0.5}Zn_{0.5}Fe_2O_4$ synthesized at 200 °C for 5 h, the diffraction angles at $2\theta = 18.25°$, 30.04°, 35.42°, 43.03°, 54.02°, 56.86°, 62.33°, and 73.92° are characteristic peaks of $Ni_{0.5}Zn_{0.5}Fe_2O_4$. The diffraction angles at $2\theta = 24.13°$, 33.08°, 40.82°, and 49.35° correspond to characteristic peaks of γ-Fe_2O_3, which indicated that $Ni_{0.5}Zn_{0.5}Fe_2O_4$ and γ-Fe_2O_3 coexisted in the sample. Curve b is XRD pattern of $Ni_{0.5}Zn_{0.5}Fe_2O_4$ synthesized at 220 °C for 5 h, the diffraction peaks of (111), (220), (311), (400), (422), (511), (531), and (533) crystal plane are indexed to pure

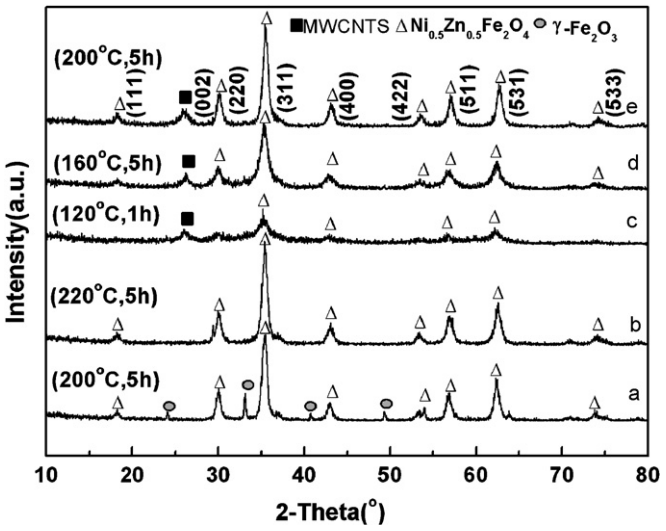

Fig. 1. XRD patterns of materials hydrothermally treated at various conditions (a) 200 °C 5 h for $Ni_{0.5}Zn_{0.5}Fe_2O_4$, (b) 220 °C 5 h for $Ni_{0.5}Zn_{0.5}Fe_2O_4$, (c) 120 °C 1 h for $Ni_{0.5}Zn_{0.5}Fe_2O_4$–MWCNTs, (d) 160 °C 5 h for $Ni_{0.5}Zn_{0.5}Fe_2O_4$–MWCNTs, and (e) 200 °C 5 h for $Ni_{0.5}Zn_{0.5}Fe_2O_4$–MWCNTs.

$Ni_{0.5}Zn_{0.5}Fe_2O_4$ phase according to the standard JCPDS (Card No. 8-234). No other peaks are detected. Based on the Scherrer equation, these XRD data, the crystallite size is estimated to be 17.9 nm using the line broadening of the (311) peak. The XRD patterns of $Ni_{0.5}Zn_{0.5}Fe_2O_4$–MWCNTs were shown in curves c–e. The diffraction peaks are assigned to MWCNTs at $2\theta = 25.86^\circ$ in these curves, indicating that the MWCNT structure is not completely changed in the process of hydrothermal treatment. These curves also show that the ferrite involved is not well crystallized when the hydrothermal temperature is below 160 °C. A good single-phase $Ni_{0.5}Zn_{0.5}Fe_2O_4$ crystals are formed, as seen in curve e, when the sample is hydrothermal treatment at 200 °C for 5 h. The size of $Ni_{0.5}Zn_{0.5}Fe_2O_4$ corresponding to (311) peak is about 17.2 nm, which is calculated in accordance to Scherrer formula. The XRD results show that hydrothermal treatment temperature of 200 °C is an appropriate reaction temperature to synthesize $Ni_{0.5}Zn_{0.5}Fe_2O_4$–MWCNTs.

Fig. 2 is an XPS spectrum of MWCNTs and $Ni_{0.5}Zn_{0.5}Fe_2O_4$–MWCNTs. This spectrum of $Ni_{0.5}Zn_{0.5}Fe_2O_4$–MWCNTs in Fig. 2(a) reveals a predominant presence of carbon, oxygen, nickel, iron, and zinc elements. Fig. 2 (b) shows C_{1s} spectra, bottom one for MWCNTs and upper one for $Ni_{0.5}Zn_{0.5}Fe_2O_4$–MWCNTs. The broad signal at 288.9 eV could result from carboxylic group, which is formed in the process of acid oxide treatment of MWCNTs. The peak at 284.6 eV could come from the carbon atoms of carbon nanotube walls. There is little energy shift between these two C_{1s} spectra indicating that the structure of nanotube walls remains unchanged during the process of coating.

Fig. 3 is FTIR spectra of $Ni_{0.5}Zn_{0.5}Fe_2O_4$ nanocrystals and $Ni_{0.5}Zn_{0.5}Fe_2O_4$/MWCNT composite, respectively.

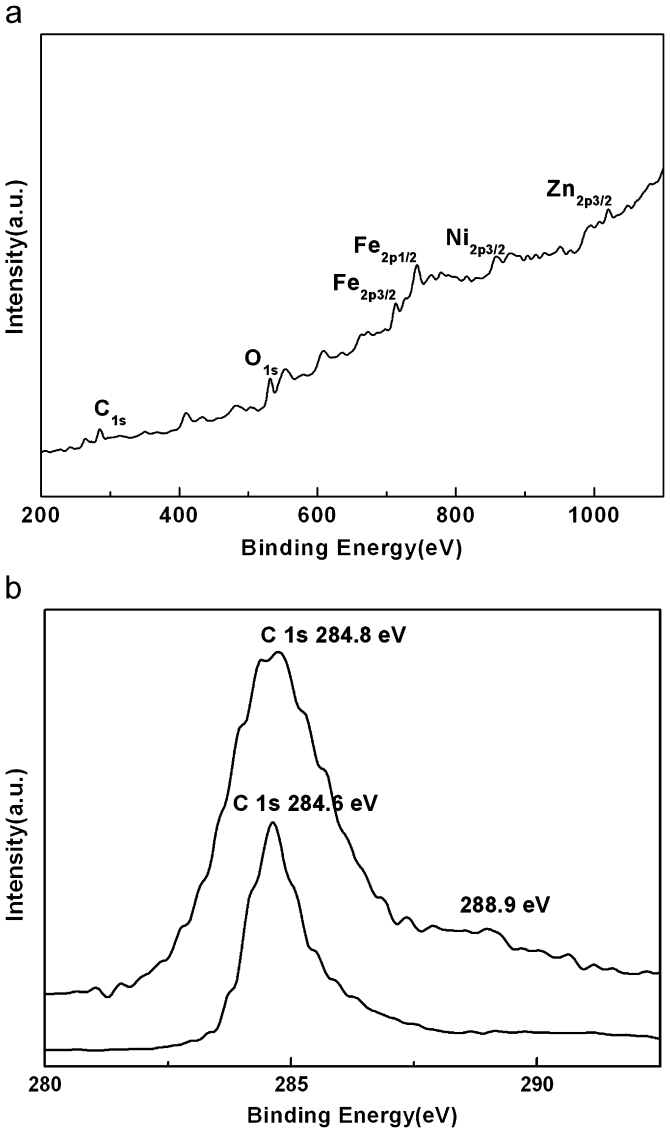

Fig. 2. The XPS spectrum of sample (a) wide-survey spectrum of $Ni_{0.5}Zn_{0.5}Fe_2O_4$–MWCNTs (b) C_{1s} spectrums of MWCNTs and $Ni_{0.5}Zn_{0.5}Fe_2O_4$–MWCNTs.

The bands at 3440 and 1632 cm^{-1} are ascribed to stretching modes and H–O–H bending vibration of free water or the water absorbed. The band at 1384 cm^{-1} is ascribed to asymmetric NO_3^- stretching vibration arising from the residual nitrate groups. The bands at 589 cm^{-1} (tetrahedral) and 425 cm^{-1} (octahedral) are characteristic bands of NiZn ferrite. The position of NiZn ferrite stretching band is shifted from small wave numbers (577 and 420 cm^{-1}) in ferrite to big wave numbers (589 and 425 cm^{-1}) in the composites, resulting from the formed interaction between NiZn ferrite and MWCNTs.

It can be observed from TEM photo in Fig. 4(a) for $Ni_{0.5}Zn_{0.5}Fe_2O_4$–MWCNTs that the diameter of MWCNTs is about 30 nm. The majority of MWCNTs surface has been attached to $Ni_{0.5}Zn_{0.5}Fe_2O_4$ nanocrystals. The structure of nanotube remains unchanged in the

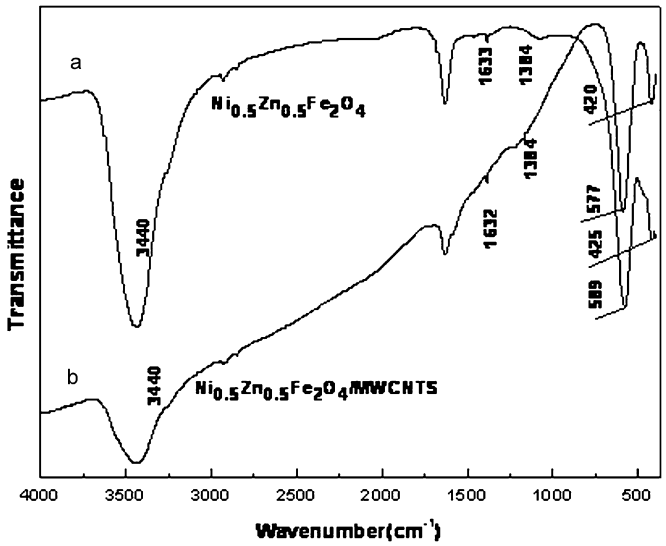

Fig. 3. FTIR spectra of as-synthesized samples (a) $Ni_{0.5}Zn_{0.5}Fe_2O_4$ nanoparticles (b) $Ni_{0.5}Zn_{0.5}Fe_2O_4$–MWCNTs.

composites. The sizes of $Ni_{0.5}Zn_{0.5}Fe_2O_4$ particles in the samples are 12–18 nm.

HRTEM micrograph of the sample prepared in Fig. 4(b) shows that this composite is consisted of the graphitized walls and $Ni_{0.5}Zn_{0.5}Fe_2O_4$ nanoparticles. The fringe spacing between two carbon layers of MWCNT is about 0.34 nm and (311) lattice spacing of $Ni_{0.5}Zn_{0.5}Fe_2O_4$ is close to 0.25 nm, as is seen in Fig. 4(b).I. The covered layer is composed of $Ni_{0.5}Zn_{0.5}Fe_2O_4$ nanocrystals having a size of 10–15 nm, which is smaller than the value calculated using Scherrer equation.

SAED patterns of $Ni_{0.5}Zn_{0.5}Fe_2O_4$–MWCNTs in Fig. 4(c) show diffusive and spotty rings clearly, indicating that the MWCNTs and $Ni_{0.5}Zn_{0.5}Fe_2O_4$ are polycrystal. A pair of arcs seen in the pattern comes from MWCNTs [34].

Mössbauer spectroscopies of $Ni_{0.5}Zn_{0.5}Fe_2O_4$–MWCNTs and $Ni_{0.5}Zn_{0.5}Fe_2O_4$ nanocrystals are shown in Fig. 5. There are a doublet and two sextet, the detailed data are listed in Table 1. The double peaks of smaller size ferrites

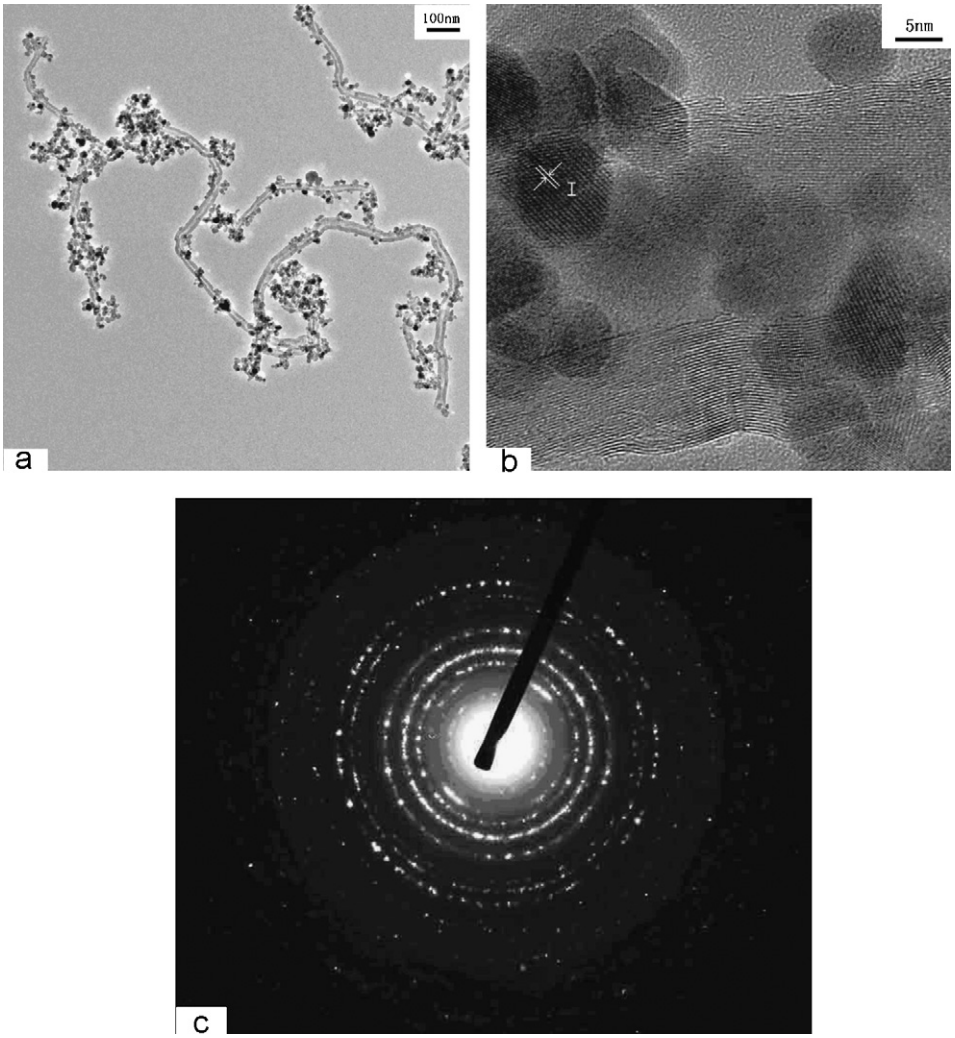

Fig. 4. (a) TEM images of Ni0.$_5$$Zn_{0.5}Fe_2O_4$–MWCNTs (b) HRTEM images $Ni_{0.5}Zn_{0.5}Fe_2O_4$–MWCNTs and (c) SAED patterns of $Ni_{0.5}Zn_{0.5}Fe_2O_4$–MWCNTs.

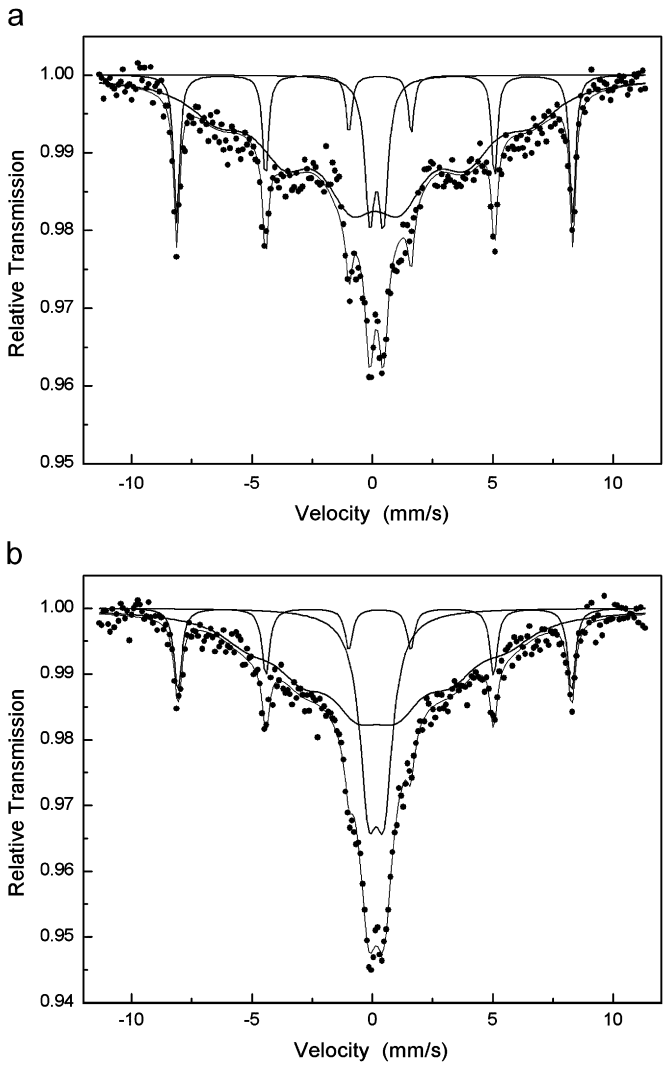

Fig. 5. Mössbauer spectroscopy of as-synthesized samples measured at room temperature (a) $Ni_{0.5}Zn_{0.5}Fe_2O_4$ nanoparticles and (b) $Ni_{0.5}Zn_{0.5}Fe_2O_4$–MWCNTs.

Table 1
Mössbauer spectroscopy parameters of the samples

Sample		H (kOe)	I.S. (mm/s)	Q.S. (mm/s)	Area
$Ni_{0.5}Zn_{0.5}Fe_2O_4$–MWCNTs	Doublet		0.34	0.64	0.248
	Sextet1	506.11	0.38	0.21	0.12
	Sextet2	330.95	0.38	0.04	0.632
$Ni_{0.5}Zn_{0.5}Fe_2O_4$	Doublet		0.35	0.56	0.098
	Sextet1	509.03	0.38	0.22	0.132
	Sextet2	403.76	0.28	0.04	0.77

obviously differ from those of bulk ferrites, which are sextet peaks. The doublets from these samples reveal a collapse of magnetic ordering due to superparamagnetic relaxation. The I.S. of the prepared composite does not exhibit a significant variation for $Ni_{0.5}Zn_{0.5}Fe_2O_4$ nanocrystals, indicating that the *s*-electron charge distribution of Fe^{3+} ions is not influenced by MWCNTs addition. It can be seen that the area of doublet absorption in the composite is about 24.8% of the total absorption, which is larger than that of $Ni_{0.5}Zn_{0.5}Fe_2O_4$ nanocrystals, indicating that more nanocrystals with a smaller size of $Ni_{0.5}Zn_{0.5}Fe_2O_4$ is formed in the reaction. The average hyperfine field of $Ni_{0.5}Zn_{0.5}Fe_2O_4$–MWCNTs increases with a decrease of $Ni_{0.5}Zn_{0.5}Fe_2O_4$ nanocrystal sizes in the influence of superparamagnetic relaxation.

Magnetic properties of $Ni_{0.5}Zn_{0.5}Fe_2O_4$–MWCNTs, $Ni_{0.5}Zn_{0.5}Fe_2O_4$, and MWCNTs were measured in fields between ± 4 kOe at room temperature. Hysteresis loops of the $Ni_{0.5}Zn_{0.5}Fe_2O_4$ and $Ni_{0.5}Zn_{0.5}Fe_2O_4$–MWCNTs are presented in Fig. 6. The magnetic parameters of $Ni_{0.5}Zn_{0.5}Fe_2O_4$–MWCNTs, $Ni_{0.5}Zn_{0.5}Fe_2O_4$, and MWCNTs are summarized in Table 2. The MWCNTs possess weak magnetic properties, perhaps attributed to the catalyst residuals and/or the nanotube used in the preparation [35]. The hysteresis loops of $Ni_{0.5}Zn_{0.5}Fe_2O_4$–MWCNTs and $Ni_{0.5}Zn_{0.5}Fe_2O_4$ are similar. The hysteresis loop of $Ni_{0.5}Zn_{0.5}Fe_2O_4$–MWCNTs exhibits a typical ferromagnetic behavior. The saturation magnetization (M_s) is found to be 28.82 emu/g, this value of M_s for $Ni_{0.5}Zn_{0.5}Fe_2O_4$–MWCNTs is considerably smaller than that of $Ni_{0.5}Zn_{0.5}Fe_2O_4$ nanocrystals (38.1 emu/g) for the non-magnetic (weak magnetic) substance of CNT existed in the composite. Compared with the value of coercivity

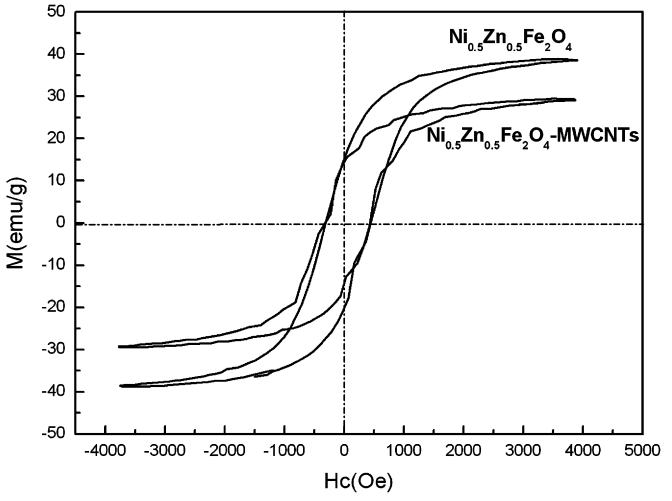

Fig. 6. Hystertsis loops of $Ni_{0.5}Zn_{0.5}Fe_2O_4$ and $Ni_{0.5}Zn_{0.5}Fe_2O_4$–MWCNTs.

Table 2
Magnetic properties of MWCNTs, $Ni_{0.5}Zn_{0.5}Fe_2O_4$–MWCNTs, and $Ni_{0.5}Zn_{0.5}Fe_2O_4$

Samples	M_s (emu/g)	M_r (emu/g)	H_c (Oe)
MWCNTs	0.17	0.038	145.33
$Ni_{0.5}Zn_{0.5}Fe_2O_4$–MWCNTs	28.82	14.25	385.98
$Ni_{0.5}Zn_{0.5}Fe_2O_4$	38.14	17.32	367.78

($H_c \approx 367.8$ Oe) of $Ni_{0.5}Zn_{0.5}Fe_2O_4$ nanocrystals, an enhancement of coercivity ($H_c \approx 386$ Oe) for $Ni_{0.5}Zn_{0.5}Fe_2O_4$–MWCNTs was observed. It is understood that the size of particles has significant influence on their magnetic properties for magnetic material. For large particles, magnetic domains are formed to reduce the static magnetic energy. The number of domains diminishes with the decreasing of the particle size. The particles turn into single domain when their sizes are below a critical radius, resulting in the increasing coercive force. This is due to vanishing of the magnetization from the movement of domain walls. The size of $Ni_{0.5}Zn_{0.5}Fe_2O_4$ nanocrystals in the composite is smaller than that of single-phase $Ni_{0.5}Zn_{0.5}Fe_2O_4$, as discussed in XRD and MS results previously. As a result, the composite has a larger coercivity than the $Ni_{0.5}Zn_{0.5}Fe_2O_4$ nanocrystals.

4. Conclusion

Novel magnetic composites of MWCNTs coated with $Ni_{0.5}Zn_{0.5}Fe_2O_4$ nanoparticles are successfully synthesized by a chemical precipitation–hydrothermal method. The composites contained $Ni_{0.5}Zn_{0.5}Fe_2O_4$ nanocrystals and MWCNTs. The hydrothermal temperature of 200 °C is an appropriate temperature to prepare high-performance $Ni_{0.5}Zn_{0.5}Fe_2O_4$–MWCNT composites, being lower than the synthesis temperature of a single-phase $Ni_{0.5}Zn_{0.5}Fe_2O_4$ nanocrystals. The size of $Ni_{0.5}Zn_{0.5}Fe_2O_4$ nanocrystals coated on the outside wall of the MWCNTs is about 15 nm. A smaller size of $Ni_{0.5}Zn_{0.5}Fe_2O_4$ nanocrystals formed in the composite than in the single-phase $Ni_{0.5}Zn_{0.5}Fe_2O_4$ resulted in the area proportion of absorption of doublet peak in the composite increased from 9.8% to 24.8% in the Mössbauer spectrums. It can be further noted that the composites exhibit satisfactory magnetic property. Particularly, the coercivity of $Ni_{0.5}Zn_{0.5}Fe_2O_4$–MWCNTs is much larger than those of other CNT magnetic composites reported in literatures [26–28]. $Ni_{0.5}Zn_{0.5}Fe_2O_4$–MWCNT magnetic composites provide an applied opportunity in the fields of electronic–magnetic nanodevices, absorbing materials, data storage systems and heterogeneous catalysis.

Acknowledgments

Acknowledgement goes to National Natural Science Foundation of China (Grant No. 50473002), Shanghai Nanotechnology Special Project (Grant No. 0359nm208), Shenzhen University Project (Grant No. 4CHQ), Cultivation Fund of the Key Scientific and Technical Innovation Project provided by the Ministry of Education of China (Grant No. 704021) for their financial supports.

References

[1] A.H. Morrish, K. Haneda, J. Appl. Phys. 52 (1981) 2496–2498.
[2] A.S. Albuquerque, J.D. Ardisson, W.A.A. Macedo, et al., J. Magn. Magn. Mater. 226–230 (2001) 1379–1381.
[3] N.A.D. Burke, H.D.H. Stöver, F.P. Dawson, Chem. Mater. 14 (2002) 4752–4761.
[4] X.Y. Zhang, Y.J. Chen, J. Magn. Magn. Mater. 270 (2004) 203–207.
[5] S.L. Kadam, C.M. Kanamadi, K.K. Patankar, B.K. Chougule, Mater. Lett. 59 (2005) 215–219.
[6] Y.K. Fetisov, A.A. Bush, K.E. Kamentsev, G. Srinivasan, Solid State Commun. 132 (2004) 319–324.
[7] C.H. Peng, H.W. Wang, S.W. Kan, M.Z. Shen, Y.M. Wei, S.Y. Chen, J. Magn. Magn. Mater. 284 (2004) 113–119.
[8] R.H. Baughman, A.A. Zakhidov, W.A. Heer, Science 297 (2002) 787–792.
[9] E.T. Thostenson, Z. Ren, T.W. Chou, Comput. Sci. Technol. 61 (2001) 1899–1912.
[10] P.K. Tyagi, M.K. Singh, M. Abha, P. Umesh, D.S. Misra, E.N. Titus, et al., Thin Solid Films 469–470 (2004) 127–130.
[11] G. Korneva, H.H. Ye, Y. Gogotsi, D. Halverson, G. Friedman, J.C. Bradley, et al., Nano Lett. 5 (2005) 879–884.
[12] L.H. Guan, Z.J. Shi, M.X. Li, Z.N. Gu, Carbon 43 (2005) 2780–2785.
[13] C. Tsang, Y.K. Chen, P.J.F. Harris, M.L.H. Green, Nature 372 (1994) 159–161.
[14] K. Nicolas, P.H. Cuong, E. Claude, G. Jean-Marc, E. Gabrielle, J.L. Marc, Carbon 42 (2004) 1395–1399.
[15] B.K. Pradhan, T. Toba, T. Kyotani, A. Tomita, Chem. Mater. 10 (1998) 2510–2515.
[16] M. Monthioux, Carbon 40 (2002) 1809–1823.
[17] Y.H. Wu, P.W. Qiao, J.J. Qiu, T.C. Chong, T.S. Low, Nano Lett. 2 (2002) 161–164.
[18] I. Mönch, A. Meye, A. Leonhardt, K. Kärmer, R. Kozhuharova, T. Gemming, et al., J. Magn. Magn. Mater. 290–291 (2005) 276–278.
[19] S.W. Liu, J. Rudolf, Carbon 43 (2005) 1550–1555.
[20] Z.Y. Sun, H.Q. Yuan, Z.M. Liu, B.X. Han, X.R. Zhang, Adv. Mater. 17 (2005) 2993–2997.
[21] H.S. Kim, S. Wolfgang, Carbon 43 (2005) 1743–1748.
[22] X.P. Gao, Y. Zhang, X. Chen, G.L. Pan, J. Yan, F. Wu, et al., Carbon 42 (2004) 47–52.
[23] L.Q. Jiang, L. Gao, Chem. Mater. 15 (2003) 2848–2853.
[24] G. Vasilios, T. Vasilios, G. Dimitrios, P. Dimitrios, Chem. Mater. 17 (2005) 1613–1617.
[25] M.A. Correa-Duarte, M. Grzelczak, V. Salgueiriño-Maceira, M. Giersig, L.M. Liz-Marzán, M. Farle, et al., J. Phys. Chem. B 109 (2005) 19060–19063.
[26] B.J. He, M. Wang, W.L. Sun, Z.Q. Shen, Mater. Chem. Phys. 95 (2006) 289–293.
[27] J. Jang, K.J. Lee, Y. Kim, Chem. Commun. 2 (2005) 3847–3849.
[28] J. Jang, H. Yoon, Adv. Mater. 5 (2003) 2088.
[29] H.Q. Cao, M.F. Zhu, Y.G. Li, J. Solid State Chem. 179 (2006) 1206–1210.
[30] S.A. Morrison, C.L. Cahill, E.E. Carpenter, S. Calvin, R. Swaminathan, M.E. McHenry, et al., J. Appl. Phys. 95 (11) (2004) 6392–6395.
[31] A. Dias, R.L. Moreira, Mater. Lett. 39 (1999) 69–76.
[32] Y.Q. Liu, L. Gao, Carbon 43 (2005) 47–52.
[33] A.E. Virden, K. O'Grady, J. Magn. Magn. Mater. 290–291 (2005) 868–870.
[34] M. Keitaro, K.P. Bhabendra, K. Takashi, T. Akira, J. Phys. Chem. B 105 (2001) 5682–5688.
[35] J.H. Wu, L.B. Kong, Appl. Phys. Lett. 84 (2004) 4956–4958.